TECHNIQUES FOR PHYSIOLOGY

Local recovery of cardiac calcium-induced calcium release interrogated by ultra-effective, two-photon uncaging of calcium

Radoslav Janicek[1] (ID), Hitesh Agarwal[2] (ID), Ana M. Gómez[3] (ID), Marcel Egger[1] (ID), Graham C. R. Ellis-Davies[2] (ID) and Ernst Niggli[1] (ID)

[1] *Department of Physiology, University of Bern, Bern, Switzerland*
[2] *Department of Neuroscience, Mount Sinai School of Medicine, New York, NY, USA*
[3] *Signaling and cardiovascular pathophysiology – UMR-S 1180, Inserm, Université Paris-Saclay, Châtenay-Malabry, France*

Edited by: Don Bers & Michael Shattock

Key points

- In cardiac myocytes, subcellular local calcium release signals, calcium sparks, are recruited to form each cellular calcium transient and activate the contractile machinery.
- Abnormal timing of recovery of sparks after their termination may contribute to arrhythmias.
- We developed a method to interrogate recovery of calcium spark trigger probabilities and their amplitude over time using two-photon photolysis of a new ultra-effective caged calcium compound.
- The findings confirm the utility of the technique to define an elevated sensitivity of the calcium release mechanism *in situ* and to follow hastened recovery of spark trigger probabilities in a mouse model of an inherited cardiac arrhythmia, which was used for validation.
- Analogous methods are likely to be applicable to investigate other microscopic subcellular signalling systems in a variety of cell types.

Abstract In cardiac myocytes Ca^{2+}-induced Ca^{2+} release (CICR) from the sarcoplasmic reticulum (SR) through ryanodine receptors (RyRs) governs activation of contraction. Ca^{2+} release occurs via subcellular Ca^{2+} signalling events, Ca^{2+} sparks. Local recovery of Ca^{2+} release depends on both SR refilling and restoration of Ca^{2+} sensitivity of the RyRs. We used two-photon (2P) photolysis of the ultra-effective caged Ca^{2+} compound BIST-2EGTA and laser-scanning confocal Ca^{2+} imaging to probe refractoriness of local Ca^{2+} release in control conditions and in the presence of cAMP or low-dose caffeine (to stimulate CICR) or cyclopiazonic acid (CPA; to slow SR refilling).

Radoslav Janicek received his PhD in animal physiology from the Comenius University in Bratislava. After a postdoctoral stay in Rutgers New Jersey Medical School in Newark, he moved to Bern to the Department of Physiology of the University of Bern. His research focuses on calcium signalling in cardiac myocytes using a combination of confocal imaging, electrophysiology techniques and photolysis of caged compounds.

Permeabilized cardiomyocytes were loaded with BIST-2EGTA and rhod-2. Pairs of short 2P photolytic pulses (1 ms, 810 nm) were applied with different intervals to test Ca^{2+} release amplitude recovery and trigger probability for the second spark in a pair. Photolytic and biological events were distinguished by classification with a self-learning support vector machine (SVM) algorithm. In permeabilized myocytes data recorded in the presence of CPA showed a lower probability of triggering a second spark compared to control or cAMP conditions. Cardiomyocytes from a mouse model harbouring the arrhythmogenic RyR^{R420Q} mutation were used for further validation and revealed a higher Ca^{2+} sensitivity of CICR. This new 2P approach provides composite information of Ca^{2+} release amplitude and trigger probability recovery reflecting both SR refilling and restoration of CICR and RyR Ca^{2+} sensitivity. It can be used to measure the kinetics of local CICR recovery, alterations of which may be related to premature heart beats and arrhythmias.

Introduction

Cardiac muscle contractions are controlled by transient elevations of the intracellular Ca^{2+} concentration in each cardiomyocyte. A large fraction of these transients is governed by Ca^{2+} released from the sarcoplasmic reticulum (SR) via Ca^{2+} release channels located on the SR membrane. These channels are ryanodine receptors (RyRs, RyR2 in the heart) and are activated by the Ca^{2+}-induced Ca^{2+} release (CICR) mechanism by Ca^{2+} entering via L-type Ca^{2+} channels (for review see Bers, 2002). SR Ca^{2+} release occurs via summation of elementary microscopic Ca^{2+} signalling events, termed Ca^{2+} sparks. While usually triggered by Ca^{2+} entry, sparks can also occur spontaneously between heartbeats.

The RyRs form tetrameric macromolecular complexes (2.2 MDa) which contain several accessory proteins (e.g. protein kinases and phosphatases), and their Ca^{2+} signalling function is regulated by multiple post-translational protein modifications, including phosphorylation of several sites, but also by oxidation (for review see Niggli *et al.* 2013). More than 200 mutations of the RyR2 have been identified, most of them resulting in a gain of function with abnormally high Ca^{2+} sensitivity. This can lead to untimely (i.e. diastolic) larger spontaneous Ca^{2+} release events, such as Ca^{2+} waves. The latter have an arrhythmogenic potential, by causing delayed afterdepolarizations. Consequently, many patients harbouring RyR2 mutations suffer from potentially life threatening catecholaminergic polymorphic ventricular tachycardias (CPVTs), often precipitated by emotional stress or physical activity.

A variety of approaches have been developed to examine the function of the RyRs from the molecular to the cellular level. For example, RyRs can be incorporated into artificial lipid bilayers to perform single channel electrophysiological studies (e.g. Cannell *et al.* 2013), while purified SR vesicles containing RyRs are amenable to a variety of biochemical functional experiments (Ferrero *et al.* 2007). This allows examination of ion binding and transport, and even estimation of RyR open probability, because ryanodine only binds to the open channels. In isolated cells, information about the RyRs and CICR can be obtained by recording transient whole-cell Ca^{2+} signals, but also by evaluating spontaneous or triggered Ca^{2+} sparks and waves. While the biochemical studies using SR vesicles usually examine the RyR function with a low temporal resolution or in the steady-state, the cellular Ca^{2+} signalling events are rapid and occur in the millisecond time domain, representing a challenge for most imaging techniques.

Analysis of spontaneous Ca^{2+} sparks provides information about RyR function at a near molecular level, while the channels are still in their normal environment within the Ca^{2+} release unit (CRU). This approach is a powerful way to understand functional alterations of the RyRs resulting, for example, from post-translational modifications or from CPVT and other RyR mutations. Unfortunately, the experimenter has very limited control over the occurrence of spontaneous Ca^{2+} sparks, and if the spark frequency is low, a reasonable analysis, which requires a substantial number of events to be evaluated, is not feasible.

Methods to overcome this experimental limitation have been developed in the past. One technique makes use of long-lasting RyR openings to a subconductance state that can be elicited by a very low dose of ryanodine (Ramay *et al.* 2011). Thereby, one channel within a RyR cluster is thought to drive repetitive Ca^{2+} sparks originating from that particular cluster. Analysis of amplitude recovery and the distribution of the intervals can be performed to extract information about the RyRs. However, this method

relies on a distinctly non-physiological stimulus regime to elicit Ca^{2+} release from the SR.

Here we present an alternative solution. Making use of the new caged Ca^{2+} compound BIST-2-EGTA (Agarwal *et al.* 2016), protocols with paired two-photon (2P) photolytic trigger pulses can be applied to elicit Ca^{2+} sparks at short to long intervals. This new caged molecule is vastly superior to previously available compounds. Importantly, the two-photon absorbance cross section is 350 Goeppert-Mayer (GM), while for DM-nitrophen it is only 0.01 GM. This allows much lower concentrations of the compound to be used, much shorter illumination times to be applied and requires dramatically reduced 2P photolytic power levels. Because of these superior features of the new compound, such paired 2P protocols can be applied, for the first time, with physiologically relevant timing (i.e. in the millisecond range). Since in confocal line scan recordings these photolytic Ca^{2+} signals have spatiotemporal features that are rather comparable to the biological Ca^{2+} sparks themselves, a machine learning approach was adopted to distinguish between the two similar events during the image analysis. This involved the use of support vector machines (SVMs), supervised learning models, which analyse data and recognize patterns. They are frequently used for classifications tasks (Noble, 2006). In this paper, we introduce this procedure and validate the technique by using pharmacological modifiers for CICR and a transgenic mouse model harbouring the arrhythmogenic RyR^{R420Q} mutation (Domingo *et al.* 2015; Yin *et al.* 2021).

Methods

Ethical approval

Housing and breeding of the mice was carried out in the departmental animal facility, with free access to rodent laboratory chow and water and a 12:12 h day–night cycle. Handling was performed with permission of the State Veterinary Administration of the Canton of Bern (BE) and in accordance with Swiss Federal Animal protection law. The animal experimentation permit (No. BE 6/2019) was issued after ethical review of our experimental and preparatory procedures, including the death of the mice (see below), by the State Committee for Animal Ethics and with endorsement by the State Veterinarian of the Canton of Bern, and after final approval by the Swiss Federal Food Safety and Veterinary Office. All experiments were carried out in accordance with the guidelines and regulations on animal experimentation of *The Journal of Physiology* (Grundy, 2015).

Animals and cardiac myocytes isolation

Ventricular myocytes were isolated from C57Bl/6 or homozygous RyR2^{R420Q} knock-in male mice, aged between 3 and 11 months (Wang *et al.* 2017) following an established protocol (Louch *et al.* 2011). Adult mice were euthanized by cervical dislocation and the hearts were excised, cannulated and retrogradely perfused on a Langendorff system. Hearts were perfused at 37°C for around 15 min with a Ca^{2+}-free modified Tyrode solution composed of (mmol/l): 140 NaCl, 5.4 KCl, 1.1 $MgCl_2$, 10 HEPES, 1 NaH_2PO_4, 10 glucose (pH 7.4). Cells were enzymatically dissociated using a cocktail of collagenase type II (160 U/ml, Allschwil, Worthington, Switzerland) and protease type XIV (0.21 U/ml, Buchs, Sigma, Switzerland). After isolation, ventricular myocytes were kept at room temperature in a modified Tyrode solution containing 250 μmol/l $CaCl_2$ and used within 6 h.

Two-photon photolysis in permeabilized cardiac myocytes

Isolated ventricular myocytes were permeabilized by exposure to β-escin for 60 s (in mmol/l: 100 potassium aspartate, 20 KCl, 3.7 $MgCl_2$, 0.5 EGTA, 10 HEPES, 0.005% β-escin; pH 7.2). Permeabilized myocytes were then placed in a recording chamber in a final solution containing (mmol/l): 120 potassium aspartate, 3 K_2ATP, 0.1 EGTA, 3 $MgCl_2$, 10 phosphocreatine, 5 U/ml creatine phosphokinase, 10 HEPES, 1 L-glutathione reduced, 0.04 $CaCl_2$, 0.05 rhod-2-K_3, 0.05 BIST-2EGTA-K_8; final $[Ca^{2+}]_i$ was 60 nmol/l, pH 7.2. Free Ca^{2+} concentration was calculated using Patcher's Power Tools package for Igor Pro (WaveMetrics, Lake Oswego, OR, USA). In pharmacological experiments 5 μmol/l cAMP, 1 μmol/l cyclopiazonic acid (CPA) or 10 mmol/l caffeine together with 20 mmol/l 2,3-butanedione 2-monoxime (BDM) was added.

A mode-locked Ti:sapphire laser was used for 2P excitation of BIST-2EGTA. The wavelength of the laser was set to 810 nm with pulse duration of $\sim$120 fs.

The power of the laser was adjusted to 20 mW by neutral density and polarizing filters and was measured at the objective focal plane by a power meter (PM200 with sensor S170C, Thorlabs, Newton, NJ, USA). The laser beam was guided to the second SIM scanner of the confocal microscope (Fluoview 1000, Olympus, Volketswil, Switzerland) operating in single point excitation mode simultaneously with the main scanner.

Pairs of photolytic pulses (Fig. 1*A*) were triggered by the confocal microscope using the Time Controller module in Fluoview 1000 software. Intra-pair interval as well as duration of individual photolytic pulses was controlled by two daisy-chained electronic shutters LS3 (Vincent Associates, Rochester, NY, USA). The duration of the individual photolytic pulse was 1 ms. The main scanner

of the confocal microscope was operating in line scan mode. To record changes in Ca^{2+} concentration rhod-2 (Biotium Inc., Hayward, CA, USA) was excited at 561 nm and detected at 585–685 nm.

All experiments were performed at room temperature ($\sim$22°C). Chemicals were purchased from Sigma-Aldrich unless stated otherwise.

Statistical analysis

Statistical significance was tested using generalized linear mixed models (Sikkel *et al.* 2017) with two levels (isolation and cell) on the whole dataset of calcium events. Pairwise comparison with Holm–Bonferroni correction was used to test significant differences among individual groups. Data are shown as means $\pm$ 95% confidence intervals estimated from mixed models or boxplots. The *N* corresponds to the number of animals, and the *n* to number of cells. In the figures, horizontal black lines indicate significance; for details see Supporting information, Statistical Summary Document. All image and statistical analyses were performed in MATLAB (R2021a, The MathWorks, Natick, MA, USA).

Results

Local Ca^{2+} events analysis and classification

Two-photon photolytic excitation allows uncaging of Ca^{2+} from the near diffraction limited volume of the exciting laser only, thereby enabling precise spatial and temporal control over the photochemical signal used to trigger the biological Ca^{2+} sparks. But the photoreleased Ca^{2+} will immediately (within less than 1 ms) spread by diffusion thereby giving rise to an expanded Ca^{2+} signal, similar to the Ca^{2+} signals of biological Ca^{2+} sparks. Therefore, a major challenge was to distinguish between Ca^{2+} released only from BIST-2EGTA and the actually triggered Ca^{2+} spark, since both signals can be very similar.

For this purpose, line scan (*x–t*) images of Ca^{2+} fluorescence recorded with rhod-2 were analysed using a custom program written in MATLAB. A train of light flashes from a mode-locked Ti:sapphire laser triggered local Ca^{2+} events from the BIST-2EGTA:Ca complex (Fig. 1*A* and *B*). These were detected by an approach developed by Bankhead *et al.* (2011). First, the fluorescence time profile was calculated by averaging a 1 μm region around the event centres, which were determined from the images filtered by a median filter (kernel (5 x 5)). This time profile was further normalized by fitting the baseline with a high order polynomial function or spline to $\Delta F/F_0$ units. After this step, individual pairs of triggered Ca^{2+} events were fitted

by the sum of model spike functions (Fig. 1*B* and *C*) (Zahradníková *et al.* 2007; Janicek *et al.* 2013). Fits of individual Ca^{2+} events were then used to estimate their parameters such as amplitude, time to peak (TTP), full duration at half maximum (FDHM), area under the fit and time constant of exponential decay (τ_{decay}). Full width at half maximum (FWHM) was estimated from the fluorescence profile, calculated by averaging a 5 ms region around the maximum in the temporal fluorescence profile of the Ca^{2+} event, fitted by a single Gaussian function.

Ca^{2+} events generated in the presence of 10 mmol/l caffeine to empty the SR and 20 mmol/l BDM were considered to be photolytic signals only (Ca^{2+} released only from BIST-2EGTA, no Ca^{2+} spark triggered) regardless of the mouse strain used (see Fig. 1*A* and *D* left panel). These purely photolytic signals still exhibited some variability which may arise from the noise in the line scan images, the kinetics of the Ca^{2+} indicator and the limited sampling frequency. Since we had these experimental examples of purely photolytic signals, we decided to describe precisely the distribution of this class (target class) and detect data from another class (biological Ca^{2+} sparks) as outliers. To do so, we trained a one-class support vector machine (OCSVM, Schölkopf *et al.* 2001) with a non-linear kernel (RBF – Gaussian radial basis function) implemented in a library for support vector machines – LIBSVM (Chang & Lin, 2011).

The performance of an OCSVM strongly depends on its hyperparameter selection which is used to control the learning process and in our case was a combination of a Gaussian kernel with width σ and the coefficient ν. ν represents an upper bound on the fraction of outliers (rejected target data) and is also the lower bound on the fraction of support vectors (Schölkopf *et al.* 2001). To tune these hyperparameters we used the self-adaptive data shifting (SDS) method proposed by Wang *et al.* (2018), which by shifting detected edge patterns can generate high quality pseudo target and outlier data. Parameters of edge detection used in SDS were extensively studied by Li & Maguire (2011) and in this work we used recommended values for threshold (0.1) and number of nearest neighbours (ceil($5 \times \ln(N)$)), where *N* is number of training samples. First, we fitted linear dimensionality reduction PCA, to measured training data (estimated parameters of Ca^{2+} events; amplitude, TTP, FDHM, FWHM, τ_{decay}, area under the fit) and extracted two principal components. Then we generated pseudo target and outlier data for our measured dataset of photolytic events (Fig. 1*E*). The OCSVM model was trained on a dataset of measured photolytic signals and validated using generated pseudo data. The best combination of hyperparameters was found using a Bayesian optimization implemented in MATLAB (function bayesopt) with a
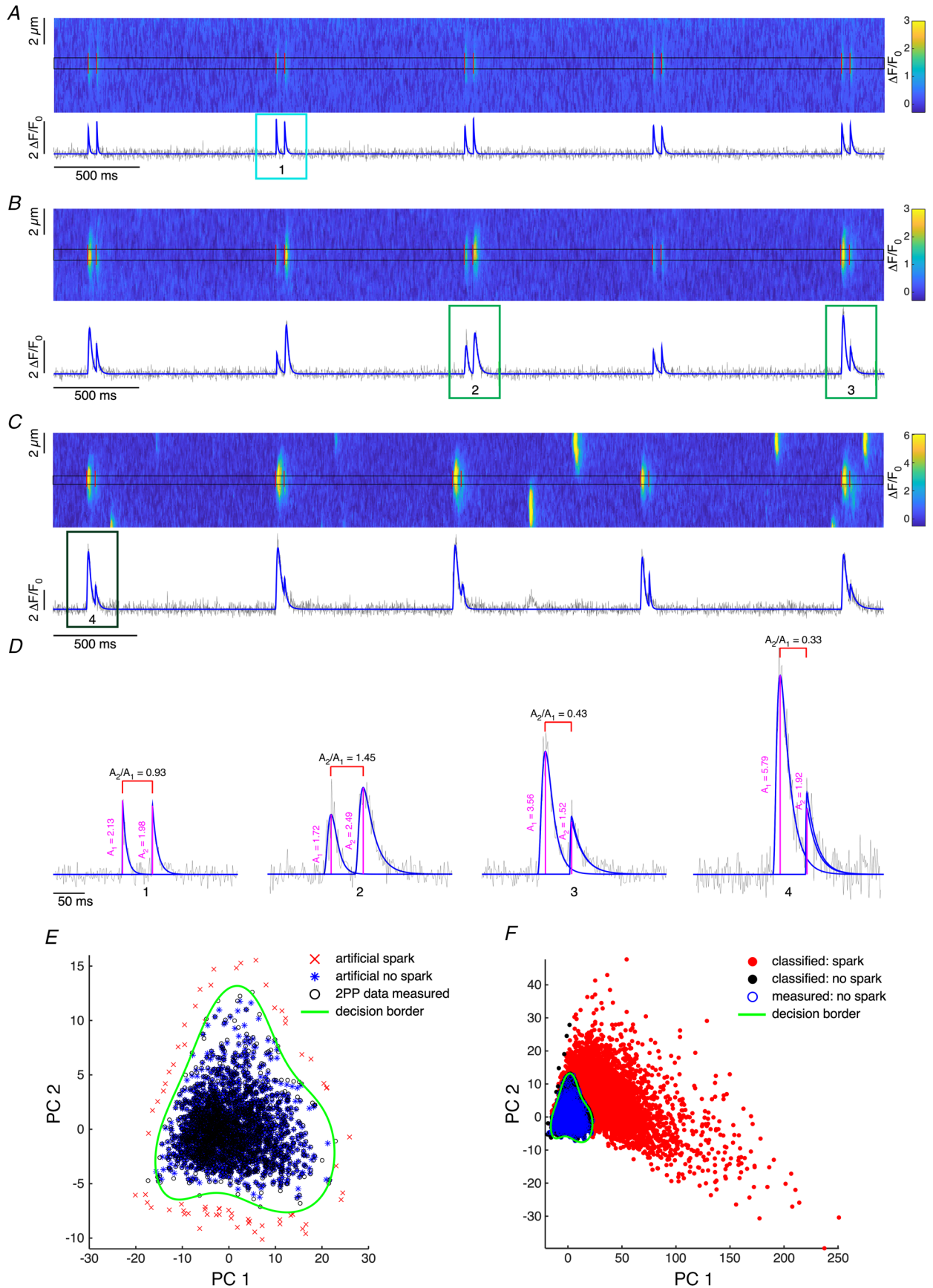
Figure 1. Two photon photolysis, Ca²⁺ event analysis and classification

A–C, line scan (*x–t*) confocal images recorded in separate permeabilized cardiac myocytes in final experimental solution in the presence of 10 mmol/l caffeine and 20 mmol/l BDM (*A*), in control conditions (*B*) and in the presence of 5 μmol/l cAMP (*C*). Vertical red lines represent positions of 2P pulses. Below each line scan is the fluorescence time profile calculated by averaging a 1 μm region (black rectangle in respective line scan) around the centres of triggered Ca²⁺ events. The blue lines are fits of events with sum of model spike functions. *D*, zoom into pairs of triggered Ca²⁺ events. Magenta lines represent detected amplitudes of events. Amplitude ratios (A_2/A_1) are calculated from individual pairs of events. *E*, scatter plot of training dataset (measured photolytic signals together with generated pseudo-data) visualized using two principal components (PC 1 and PC 2; total variance explained by two principal components was 94.6%). Green line represents decision border of trained OCSVM classifier (σ = 0.005183, ν = 0.002441). *F*, scatter plot showing classification of all measured events using the trained OCSVM classifier.

Matthews correlation coefficient (MCC; Matthews, 1975; Chicco & Jurman, 2020) as evaluation metric. The best trained classifier was then used to classify all measured events as similar (i.e. 'no spark') or different to the training set (i.e. 'spark', Fig. 1F). Very small and short Ca²⁺ events with amplitude $<0.5 \Delta F/F_0$ and FDHM <5 ms were also labelled as 'no spark'.

First triggered sparks in pairs

After classification, from all first triggered Ca²⁺ events by 2P photolysis of BIST-2ETGA, the probability of triggering a Ca²⁺ spark in wild-type (WT) and R420Q homozygous cardiomyocytes were calculated (Fig. 2*A*). In control conditions we observed a higher chance
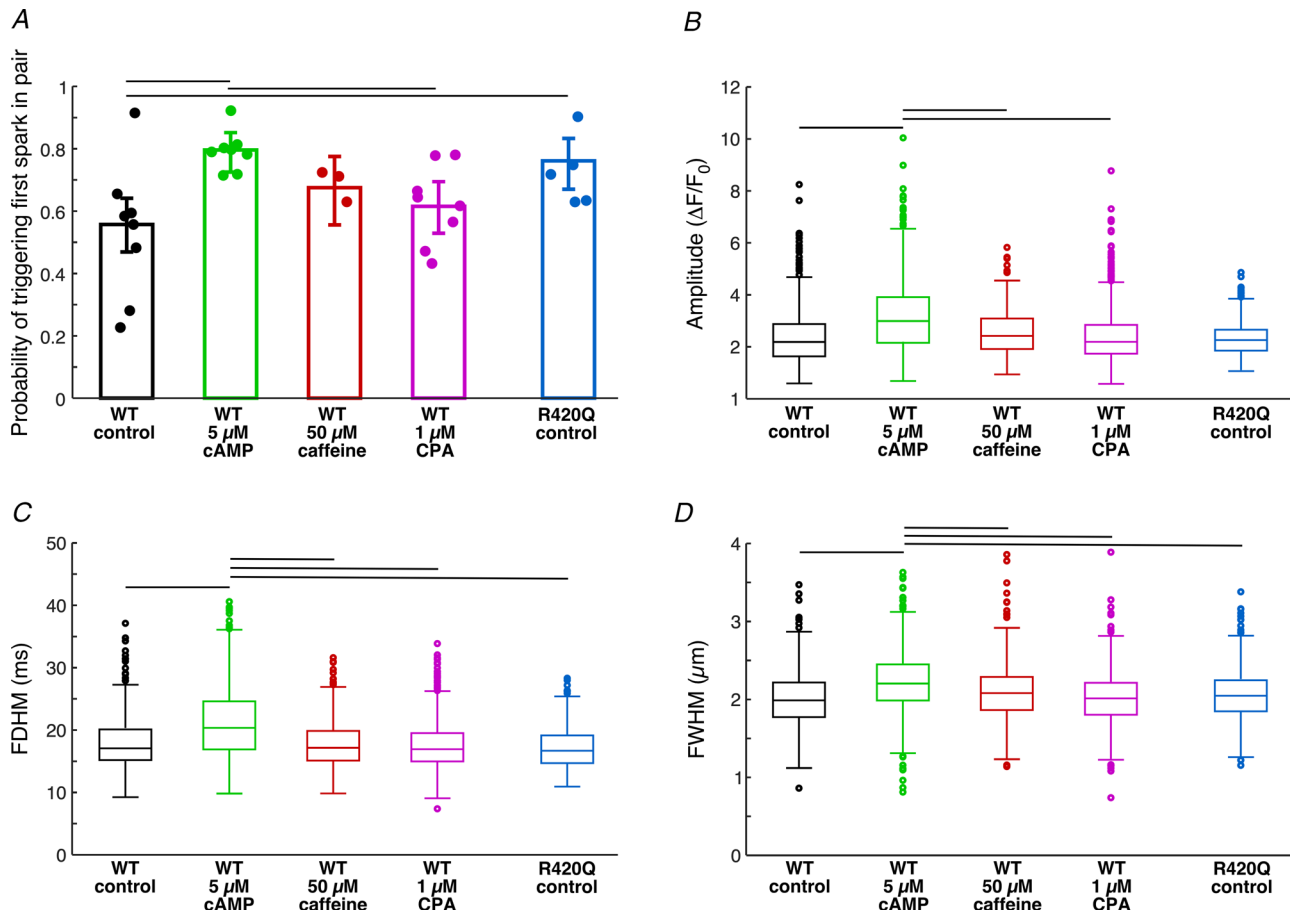

Figure 2. Triggered first Ca²⁺ sparks in pair

A, probability of triggering Ca²⁺ spark with 2P photolysis of BIST-2EGTA. Data are shown as means ± 95% confidence intervals; individual points represent average per animal. *B–D*, estimated parameters of first triggered Ca²⁺ sparks in WT and in mutant cells. R420Q control: *N* = 5, *n* = 17, first events = 710, first Ca²⁺ sparks = 511. WT control: *N* = 8, *n* = 26, first events = 1315, first Ca²⁺ sparks = 725; cAMP: *N* = 8, *n* = 24, first events = 815, first Ca²⁺ sparks = 637; caffeine: *N* = 3, *n* = 12, first events = 666, first Ca²⁺ sparks = 458; CPA: *N* = 8, *n* = 25, first events = 1452, first Ca²⁺ sparks = 867. Horizontal black lines represent significant difference, *P* < 0.05.

to trigger a Ca^{2+} spark in cells from R420Q myocytes than in WT cells ($P = 0.00141$). In WT cells, in the presence of 5 μmol/l cAMP there was a significantly higher chance of triggering a Ca^{2+} spark than in control condition ($P = 4.8 \times 10^{-6}$) or in the presence of 1 μmol/l CPA ($P = 0.00034$). We observed an increase of probability of triggering Ca^{2+} spark in the presence of 50 μmol/l caffeine, when compared to control conditions in WT animals, but it was not significant ($P = 0.0966$). Triggered Ca^{2+} sparks in WT cells had significantly higher amplitudes in the presence of 5 μmol/l cAMP than when exposed to 1 μmol/l CPA ($P = 1.35 \times 10^{-9}$), to 50 μmol/l caffeine ($P = 0.00225$) or in control conditions ($P = 1.21 \times 10^{-9}$, Fig. 2B). Ca^{2+} sparks in WT animal in the presence of cAMP had also significantly longer duration ($P = 1.4 \times 10^{-16}$ *vs*. CPA, $P = 1.4 \times 10^{-14}$ *vs*. control, $P = 2.9 \times 10^{-10}$ *vs*. 50 μmol/l caffeine, Fig. 2C) and were wider ($P = 9.8 \times 10^{-11}$ *vs*. CPA, $P = 9.3 \times 10^{-12}$ *vs*. control, $P = 3.5 \times 10^{-6}$ *vs*. 50 μmol/l caffeine, Fig. 2D). There was no significant difference in parameters of triggered sparks in control conditions between WT and R420Q animals.

These observations are compatible with the notion that the CICR and RyRs in R420Q myocytes have a slightly elevated Ca^{2+} sensitivity, consistent with the overall gain of function conferred by this genotype (Wang *et al.* 2017; Yin *et al.* 2021). Similarly, the activation of protein kinase A (PKA) in the presence of cAMP is expected to increase the RyR Ca^{2+} sensitivity. This may result from both the phosphorylation of the RyRs and the stimulation of the SERCA (after phosphorylation of phospholamban). In contrast, slowing down the SERCA with a low concentration of the SERCA inhibitor CPA (to minimize SR Ca^{2+} depletion) did not significantly affect the first Ca^{2+} release in a pair (but altered the second spark, presumably by slowing down SR refilling, see below).

Second triggered sparks in pairs

The second event in a pair provides information about the recovery of the local Ca^{2+} release mechanism from termination of the first event in a pair. Recovery will depend on a variety of factors, mainly on local refilling of the SR via intra-SR Ca^{2+} diffusion and somewhat on SERCA activity, but also on recovery of the RyRs themselves from their inactivation (Szentesi *et al.* 2004; Sobie *et al.* 2005; Ramay *et al.* 2011; Brunello *et al.* 2013; Poláková *et al.* 2015; Manno *et al.* 2017). Local recovery of CICR was tested in control conditions, in the presence of 5 μmol/l cAMP, 50 μmol/l caffeine or 1 μmol/l CPA in WT and in control conditions in R420Q cells. Only pairs of events in which a first spark was triggered were considered. We observed a trend for an increased probability of triggering a second spark in a pair in R420Q cells in control condition and also in WT cells in the presence of 5 μmol/l cAMP (Fig. 3A). In pairs of Ca^{2+} evens, where two biological Ca^{2+} sparks were triggered, we calculated spark amplitude recovery at different intra-pair intervals (Fig. 3B).

The recovery of the CICR after the first activation and inactivation is a complex phenomenon. Our data show that mechanisms making the CICR and the RyRs more Ca^{2+} sensitive (e.g. cAMP and the R420Q mutation) generally accelerate the recovery and lead to higher trigger probabilities. However, in the case of cAMP, stimulation of the SERCA and thus more rapid SR refilling may also contribute to the faster recovery. This is underscored by the observation that the SERCA inhibitor CPA slows down and reduces the recovery. The SERCA stimulation may also explain the larger amplitude of these release signals, resulting from a higher SR Ca^{2+} load. The longer spark duration in cAMP, despite SERCA stimulation, may result from spurious RyR openings during the spark decline. Differences in apparent Ca^{2+} sensitivities of CICR and the RyRs could also arise from functional or ultrastructural remodelling occurring as an adaptive process in the transgenic R420Q cardiomyocytes.

Discussion

The analysis of spontaneous Ca^{2+} sparks occurring during diastole allows examination of function of RyRs on the near molecular level *in situ* and in live cells. However, one has little or no control regarding the timing and location of these random and accidental events. This limitation can be partly overcome by triggering these events by 2P photolysis of caged Ca^{2+}. In this work we present a novel approach for measuring the Ca^{2+} sensitivity of CICR and ryanodine receptors using a recently developed ultra-effective Ca^{2+} caged compound (Agarwal *et al.* 2016). In permeabilized cardiomyocytes precise spatiotemporal control over Ca^{2+} release from the SR allowed us to determine Ca^{2+} sensitivity of CICR and the RyRs as well as the trigger probability of a second spark, which is a parameter for the recovery of the RyRs after termination of the previous release.

Triggering Ca^{2+} sparks with 2P photolysis on a physiologically relevant time scale required the development of a new caged Ca^{2+} compound with a large 2P absorption cross-section. We took advantage of knowledge gained from structure–activity relationships gained for 2P-induced fluorescence from extended pi-electron systems (Albota *et al.* 1998; Rumi *et al.* 2008), and applied it to Ca^{2+} uncaging by making BIST-2EGTA (Agarwal *et al.* 2016). The core chromophore has a 2P cross-section in the 350–775 GM range, significantly larger than our previous Ca^{2+} cages (range 0.01–0.6 GM

(DelPrincipe *et al.* 1999; Momotake *et al.* 2006)). Since Ca^{2+} is photoreleased in less than 1 ms, 2P irradiation can serve as a photochemical trigger with near physiological characteristics for Ca^{2+}-regulated events such as Ca^{2+} sparks (Wang *et al.* 2001). This was not possible with previously used caged Ca^{2+} compounds, as the low 2P cross-section meant significantly longer pulse durations (30–50 ms) were required to elicit any Ca^{2+} release from the SR. Such photolytic protocols even outlasted the typical duration of the sparks themselves and thus were not suitable for triggering pairs of Ca^{2+} sparks with intrapair intervals of less than 200 ms (Lipp & Niggli, 1998; DelPrincipe *et al.* 1999; Lindegger & Niggli, 2005; Ellis-Davies, 2020). Further, we note the exceptional

2P cross-section of BIST allowed us to use much lower concentrations of BIST-2EGTA (0.05 mmol/l) compared to simpler nitro-aromatic caged Ca^{2+} compounds such as DM-nitrophen (up to 10 mmol/l was required).

To use of this new approach really effectively, several problems needed to be overcome. Separation between classes of purely photolytic events and true triggered Ca^{2+} sparks is challenging due to overlapping distributions of several parameters of these events (Fig. 1*E* and *F*), complicated by the fact that we have a clear identification (even though based on multiple signal parameters) only for one class, for pure photolytic events measured in the presence of 10 mmol/l caffeine and 20 mmol/l BDM (Fig. 1*A*). To overcome this obstacle, we used a one-class
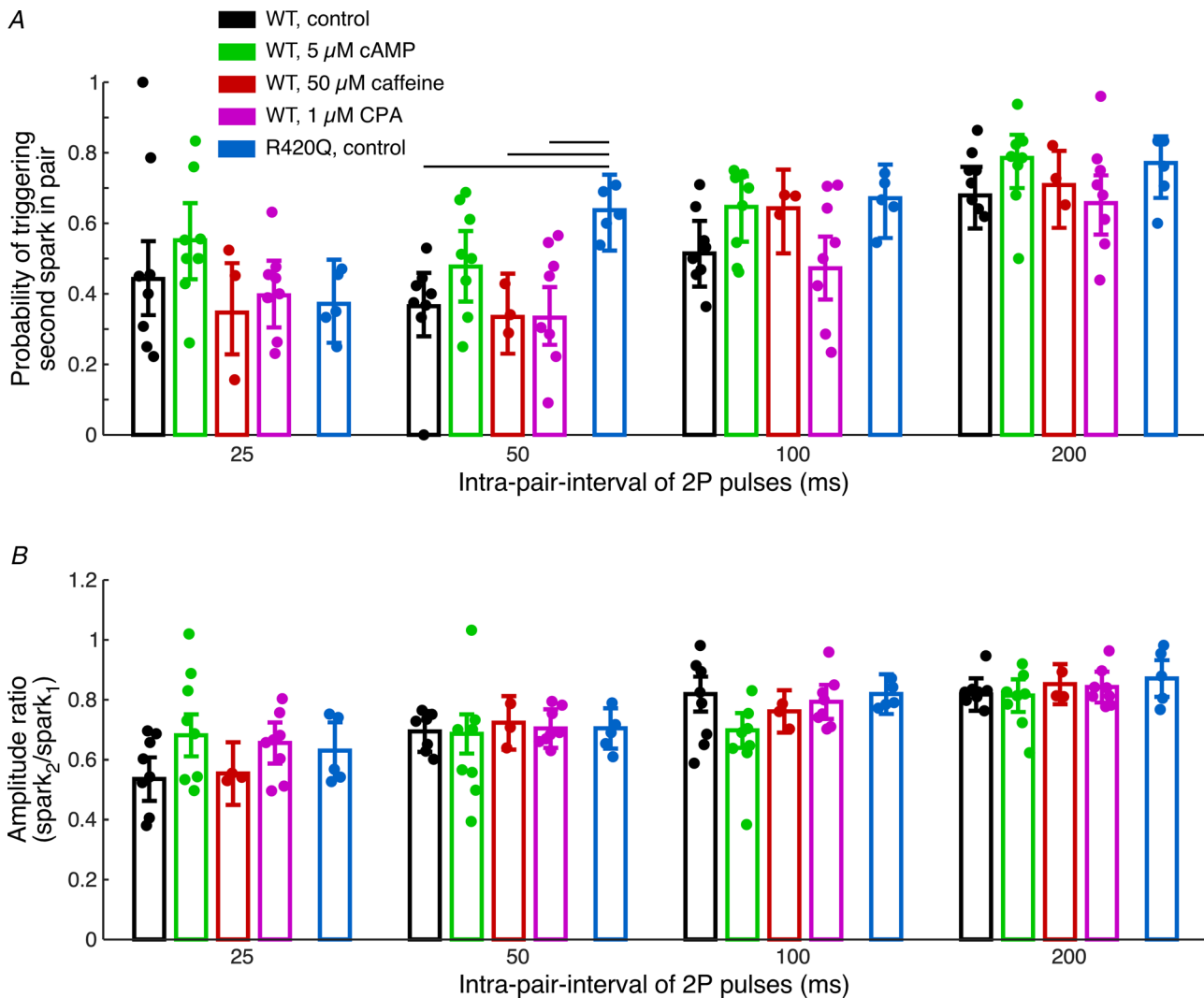

Figure 3. Triggered second Ca^{2+} spark in a pair
A, probability of triggering of a second spark in a pair at different intra-pair intervals. *B*, amplitude recovery of triggered Ca^{2+} sparks at different intra-pair intervals. Data are shown as means ± 95% confidence intervals; individual points represent average per animal. R420Q control: $N = 5$, $n = 14$–17. WT control: $N = 8$, $n = 19$–25; cAMP: $N = 8$, $n = 19$–23; caffeine: $N = 3$, $n = 10$–12; CPA: $N = 8$, $n = 20$–25. For detailed numbers of recorded Ca^{2+} events see Supporting information, Supplemental Table 1. Horizontal black lines represent significant difference, $P < 0.05$.

support vector machine (OCSVM) as a technique to precisely describe data from one class (pure photolytic signals only) and treated other signals as outliers (corresponding to Ca^{2+} sparks). The main problem with using an OCSVM is the choice of hyperparameters (σ and ν) of the classifier, which are used to control the learning process. Simple use of Ca^{2+} events with very different parameters such as photolytic signals (median of parameters of photolytic signals + 3 × median absolute deviation) was not sufficient to find a reasonable hyperplane to separate these two classes of Ca^{2+} events. To overcome this, we adopted a technique of self-adaptive data shifting (Fig. 1*E*) to create high quality and reproducible outliers (as representation of the Ca^{2+} spark class), which were then used to tune the hyperparameters of the classifier using a Mathews correlation coefficient (MCC) as metric. The MCC was preferred over the f1 score, which is a harmonic mean of the precision and recall, due to better performance in binary classification in highly imbalanced classes (Chicco & Jurman, 2020).

It was shown that each Ca^{2+} release event, either local or cell-wide, induces refractoriness. The time course of Ca^{2+} spark recovery from refractoriness depends on a variety of parameters, such as sensitivity of ryanodine receptors to cytosolic Ca^{2+} and local sarcoplasmic reticulum refilling (Terentyev *et al.* 2002; Szentesi *et al.* 2004; Sobie *et al.* 2005; Picht *et al.* 2011; Ramay *et al.* 2011; Poláková *et al.* 2015). In the literature, multiple mechanisms have been proposed to explain refractoriness and termination of Ca^{2+} release. The most recent ones are 'induction decay' (Cannell *et al.* 2013; Laver *et al.* 2013) or 'pernicious attrition' (Gillespie & Fill, 2013), which provide adequate explanations for termination of CICR. Briefly, the decline in $[Ca^{2+}]_{SR}$ results in a decrease of release flux during a Ca^{2+} spark, which cause the decrease of local cytoplasmic $[Ca^{2+}]$ in the dyad, resulting in a prolongation of closed time of RyRs. With RyR closed times getting longer, the probability of opening/re-opening of RyRs within a cluster decreases and CICR becomes unlikely to continue. This process may be also modulated by many different factors from the cytosolic side, which include Ca^{2+}, calmodulin and post-translational modification of RyRs (phosphorylation, oxidation). From the SR luminal side there are findings suggesting direct Ca^{2+} modulation of RyRs (Jiang *et al.* 2007) or through luminal Ca^{2+} sensors (e.g. calsequestrin; Terentyev *et al.* 2002; Manno *et al.* 2017). Impaired (shortened) refractoriness, as in the case of mutation of R420Q ryanodine receptors (Figs 2*A* and 3*A*), might lead to arrhythmogenic diastolic Ca^{2+} releases (Lopez *et al.* 2020; Yin *et al.* 2021). PKA stimulation by cAMP increased the probability of triggering of Ca^{2+} sparks (Figs 2*A* and 3*A*), which agrees with results of spark recovery analysis using the 'ryanodine method' (Sobie *et al.* 2005) in the presence of isoproterenol (Ramay *et al.* 2011; Poláková *et al.* 2015;

Potenza *et al.* 2019). Our analysis of Ca^{2+} spark amplitude recovery did not show any significant difference resulting from pharmacological interventions or when compared to the RyR CPVT mutation (Fig. 3*B*). A reason for this might be that the real amplitude of triggered Ca^{2+} spark is partly masked by Ca^{2+} release from photolysed BIST-2EGTA. This situation is a limitation of the 2P approach and might happen when the amplitude of triggered Ca^{2+} spark is considerably smaller than amplitude of Ca^{2+} released from caged compound, which might explain discrepancies in Ca^{2+} spark amplitude recovery observed by the 'ryanodine method'.

It is possible that due to the complex geometry and distribution of Ca^{2+} release units in cardiac myocytes (Galice *et al.* 2018; Jayasinghe *et al.* 2018; Kolstad *et al.* 2018; Sheard *et al.* 2019; Shen *et al.* 2019; Asghari *et al.* 2020), we might trigger Ca^{2+} releases from multiple CRUs during the 2P stimulus protocol. This is due to the fact that in our case the diffraction limited 2P volume is less than 0.2 fl (60 × objective with NA = 1.20, $\lambda_{2P} = 810$ nm) with $\sim$1 μm in axial and $\sim$0.5 μm in lateral dimension (Brown *et al.* 1999; Zipfel *et al.* 2003; Rubart, 2004). However, a significant advantage compared to the analysis of spontaneous Ca^{2+} sparks is the fact that we are exclusively recording Ca^{2+} events from the focal plane. Furthermore, we are not limited by the duration of these experiments, as in the case of the 'ryanodine method'. In the presence of low-dose ryanodine, the appearance of long lasting sparks (RyRs in sub-conductance states or multiple ryanodine molecules bound to RyR) is often observed after $\sim$10 min and therefore the duration of such recordings is somewhat limited (Sobie *et al.* 2005; Ramay *et al.* 2011). Another convenience of the photolytic approach is that we have perfect control over timing and location of the 2P pulses to trigger Ca^{2+} events. There is no need for a time-consuming search for repetitive sparks in cells, which might be challenging especially in conditions with a low probability of observing repetitive sparks (e.g. in the presence of Ca^{2+} release blockers). These advantages are analogous to the use of 2P uncaging of glutamate at dendritic spines (Matsuzaki *et al.* 2001), when compared to evoked release (Sabatini & Svoboda, 2000). The latter is really limited by release probability, whereas uncaging completely bypasses this restriction, allowing pure postsynaptic effects to be probed with 1 to 1 certainty (Ellis-Davies, 2018).

In summary we introduce an experimental method which provides composite information of Ca^{2+} release probability and amplitude recovery in cardiomyocytes reflecting both SR refilling and restoration of Ca^{2+} sensitivity. More broadly, we have established that BIST-2EGTA can be used as an extremely effective source of photoreleased Ca^{2+}, as very short pulses of light (1 ms) and low powers (20 mW from a mode-locked Ti:sapphire laser) from low concentrations of the probe

(only 50 μmol/L) can induce Ca^{2+}-induced physiological responses that are indistinguishable from the natural events. Since Ca^{2+} is a ubiquitous second messenger in many cell types, our current work with BIST-2EGTA indicates that new avenues of optical physiology can be examined for the first time.

References

Agarwal HK, Janicek R, Chi SH, Perry JW, Niggli E & Ellis-Davies GCR (2016). Calcium uncaging with visible light. *J Am Chem Soc* **138**, 3687–3693.

Albota M, Beljonne D, Brédas JL, Ehrlich JE, Fu JY, Heikal AA, Hess SE, Kogej T, Levin MD, Marder SR, McCord-Maughon D, Perry JW, Röckel H, Rumi M, Subramaniam G, Webb WW, Wu XL & Xu C (1998). Design of organic molecules with large two-photon absorption cross sections. *Science* **281**, 1653–1656.

Asghari P, Scriven DR, Ng M, Panwar P, Chou KC, Van Petegem F & Moore ED (2020). Cardiac ryanodine receptor distribution is dynamic and changed by auxiliary proteins and post-translational modification. *Elife* **9**, 40.

Bankhead P, Scholfield CN, Curtis TM & McGeown JG (2011). Detecting Ca^{2+} sparks on stationary and varying baselines. *Am J Physiol Cell Physiol* **301**, C717–C728.

Bers DM (2002). Cardiac excitation-contraction coupling. *Nature* **415**, 198–205.

Brown EB, Shear JB, Adams SR, Tsien RY & Webb WW (1999). Photolysis of caged calcium in femtoliter volumes using two-photon excitation. *Biophys J* **76**, 489–499.

Brunello L, Slabaugh JL, Radwanski PB, Ho HT, Belevych AE, Lou Q, Chen H, Napolitano C, Lodola F, Priori SG, Fedorov VV, Volpe P, Fill M, Janssen PML & Györke S (2013). Decreased RyR2 refractoriness determines myocardial synchronization of aberrant Ca^{2+} release in a genetic model of arrhythmia. *Proc Natl Acad Sci U S A* **110**, 10312–10317.

Cannell MB, Kong CHT, Imtiaz MS & Laver DR (2013). Control of sarcoplasmic reticulum Ca^{2+} release by stochastic RyR gating within a 3D model of the cardiac dyad and importance of induction decay for CICR termination. *Biophys J* **104**, 2149–2159.

Chang C-C & Lin C-J (2011). LIBSVM: A library for support vector machines. *ACM Trans Intell Syst Technol* **2**, 1–27.

Chicco D & Jurman G (2020). The advantages of the Matthews correlation coefficient (MCC) over F1 score and accuracy in binary classification evaluation. *BMC Genomics* **21**, 6.

DelPrincipe F, Egger M, Ellis-Davies GCR & Niggli E (1999). Two-photon and UV-laser flash photolysis of the Ca^{2+} cage, dimethoxynitrophenyl-EGTA-4. *Cell Calcium* **25**, 85–91.

Domingo D, López-Vilella R, Arnau MÁ, Cano Ó, Fernández-Pons E & Zorio E (2015). A new mutation in the ryanodine receptor 2 gene (RYR2 C2277R) as a cause catecholaminergic polymorphic ventricular tachycardia. *Rev Espanola Cardiol Engl Ed* **68**, 71–73.

Ellis-Davies GCR (2018). Two-photon uncaging of glutamate. *Front Synaptic Neurosci* **10**, 48.

Ellis-Davies GCR (2020). Useful caged compounds for cell physiology. *ACC Chem Res* **53**, 1593–1604.

Ferrero P, Said M, Sánchez G, Vittone L, Valverde C, Donoso P, Mattiazzi A & Mundiña-Weilenmann C (2007). Ca^{2+}/calmodulin kinase II increases ryanodine binding and Ca^{2+}-induced sarcoplasmic reticulum Ca^{2+} release kinetics during β-adrenergic stimulation. *J Mol Cell Cardiol* **43**, 281–291.

Galice S, Xie Y, Yang Y, Sato D & Bers DM (2018). Size matters: ryanodine receptor cluster size affects arrhythmogenic sarcoplasmic reticulum calcium release. *J Am Heart Assoc* **7**, e008724.

Gillespie D & Fill M (2013). Pernicious attrition and inter-RyR2 CICR current control in cardiac muscle. *J Mol Cell Cardiol* **58**, 53–58.

Grundy D (2015). Principles and standards for reporting animal experiments in *The Journal of Physiology* and *Experimental Physiology*. *J Physiol* **593**, 2547–2549.

Janicek R, Hotka M, Zahradníková A Jr, Zahradníková A & Zahradník I (2013). Quantitative analysis of calcium spikes in noisy fluorescent background. *PLoS One* **8**, e64394.

Jayasinghe I, Clowsley AH, Lin R, Lutz T, Harrison C, Green E, Baddeley D, Di Michele L & Soeller C (2018). True molecular scale visualization of variable clustering properties of ryanodine receptors. *Cell Rep* **22**, 557–567.

Jiang D, Chen W, Wang R, Zhang L & Chen SRW (2007). Loss of luminal Ca^{2+} activation in the cardiac ryanodine receptor is associated with ventricular fibrillation and sudden death. *Proc Natl Acad Sci U S A* **104**, 18309–18314.

Kolstad TR, van den Brink J, MacQuaide N, Lunde PK, Frisk M, Aronsen JM, Norden ES, Cataliotti A, Sjaastad I, Sejersted OM, Edwards AG, Lines GT & Louch WE (2018). Ryanodine receptor dispersion disrupts Ca^{2+} release in failing cardiac myocytes. *Elife* **7**, 252.

Laver DR, Kong CHT, Imtiaz MS & Cannell MB (2013). Termination of calcium-induced calcium release by induction decay: an emergent property of stochastic channel gating and molecular scale architecture. *J Mol Cell Cardiol* **54**, 98–100.

Li Y & Maguire L (2011). Selecting critical patterns based on local geometrical and statistical information. *IEEE Trans Pattern Anal Mach Intell* **33**, 1189–1201.

Lindegger N & Niggli E (2005). Paradoxical SR Ca^{2+} release in guinea-pig cardiac myocytes after β-adrenergic stimulation revealed by two-photon photolysis of caged Ca^{2+}. *J Physiol* **565**, 801–813.

Lipp P & Niggli E (1998). Fundamental calcium release events revealed by two-photon excitation photolysis of caged calcium in guinea-pig cardiac myocytes. *J Physiol* **508** 801–809.

Lopez RJ, Fernandez-Tenorio M, Janicek R, Gomez AM & Niggli E (2020). SERCA stimulation triggers arrhythmogenic Ca^{2+} events in mouse cardiomyocytes harboring the $RyR2^{R420Q+/-}$ mutation. *Biophys J* **118**, 254a.

Louch WE, Sheehan KA & Wolska BM (2011). Methods in cardiomyocyte isolation, culture, and gene transfer. *J Mol Cell Cardiol* **51**, 288–298.

Manno C, Figueroa LC, Gillespie D, Fitts R, Kang C, Franzini-Armstrong C & Rios E (2017). Calsequestrin depolymerizes when calcium is depleted in the sarcoplasmic reticulum of working muscle. *Proc Natl Acad Sci U S A* **114**, E638–E647.

Matsuzaki M, Ellis-Davies GCR, Nemoto T, Miyashita Y, Iino M & Kasai H (2001). Dendritic spine geometry is critical for AMPA receptor expression in hippocampal CA1 pyramidal neurons. *Nat Neurosci* **4**, 1086–1092.

Matthews BW (1975). Comparison of the predicted and observed secondary structure of T4 phage lysozyme. *Biochim Biophys Acta* **405**, 442–451.

Momotake A, Lindegger N, Niggli E, Barsotti RJ & Ellis-Davies GCR (2006). The nitrodibenzofuran chromophore: a new caging group for ultra-efficient photolysis in living cells. *Nat Methods* **3**, 35–40.

Niggli E, Ullrich ND, Gutierrez D, Kyrychenko S, Poláková E & Shirokova N (2013). Posttranslational modifications of cardiac ryanodine receptors: Ca^{2+} signaling and EC-coupling. *Biochim Biophys Acta* **1833**, 866–875.

Noble WS (2006). What is a support vector machine? *Nat Biotechnol* **24**, 1565–1567.

Picht E, Zima AV, Shannon TR, Duncan AM, Blatter LA & Bers DM (2011). Dynamic calcium movement inside cardiac sarcoplasmic reticulum during release. *Circ Res* **108**, 847–856.

Poláková E, Illaste A, Niggli E & Sobie EA (2015). Maximal acceleration of Ca^{2+} release refractoriness by β-adrenergic stimulation requires dual activation of kinases PKA and CaMKII in mouse ventricular myocytes. *J Physiol* **593**, 1495–1507.

Potenza DM, Janicek R, Fernandez-Tenorio M, Camors E, Ramos-Mondragón R, Valdivia HH & Niggli E (2019). Phosphorylation of the ryanodine receptor 2 at serine 2030 is required for a complete β-adrenergic response. *J Gen Physiol* **151**, 131–145.

Ramay HR, Liu OZ & Sobie EA (2011). Recovery of cardiac calcium release is controlled by sarcoplasmic reticulum refilling and ryanodine receptor sensitivity. *Cardiovasc Res* **91**, 598–605.

Rubart M (2004). Two-photon microscopy of cells and tissue. *Circ Res* **95**, 1154–1166.

Rumi M, Barlow S, Wang J, Perry JW & Marder SR (2008). Two-photon absorbing materials and two-photon-induced chemistry. In Photoresponsive Polymers I, Advances in Polymer Science Vol. 213, ed. Marder SR & Lee KS, pp. 1–95. Springer, Berlin, Heidelberg. https://link.springer.com/chapter/10.1007/12_2008_133.

Sabatini BL & Svoboda K (2000). Analysis of calcium channels in single spines using optical fluctuation analysis. *Nature* **408**, 589–593.

Schölkopf B, Platt JC, Shawe-Taylor J, Smola AJ & Williamson RC (2001). Estimating the support of a high-dimensional distribution. *Neural Comput* **13**, 1443–1471.

Sheard TMD, Hurley ME, Colyer J, White E, Norman R, Pervolaraki E, Narayanasamy KK, Hou Y, Kirton HM, Yang Z, Hunter L, Shim J-U, Clowsley AH, Smith AJ, Baddeley D, Soeller C, Colman MA & Jayasinghe I (2019). Three-dimensional and chemical mapping of intracellular signaling nanodomains in health and disease with enhanced expansion microscopy. *ACS Nano* **13**, 2143–2157.

Shen X, van den Brink J, Hou Y, Colli D, Le C, Kolstad TR, MacQuaide N, Carlson CR, Kekenes Huskey PM, Edwards AG, Soeller C & Louch WE (2019). 3D dSTORM imaging reveals novel detail of ryanodine receptor localization in rat cardiac myocytes. *J Physiol* **597**, 399–418.

Sikkel MB, Francis DP, Howard J, Gordon F, Rowlands C, Peters NS, Lyon AR, Harding SE & MacLeod KT (2017). Hierarchical statistical techniques are necessary to draw reliable conclusions from analysis of isolated cardiomyocyte studies. *Cardiovasc Res* **113**, 1743–1752.

Sobie EA, Song L-S & Lederer WJ (2005). Local recovery of Ca^{2+} release in rat ventricular myocytes. *J Physiol* **565**, 441–447.

Szentesi P, Pignier C, Egger M, Kranias EG & Niggli E (2004). Sarcoplasmic reticulum Ca^{2+} refilling controls recovery from Ca^{2+}-induced Ca^{2+} release refractoriness in heart muscle. *Circ Res* **95**, 807–813.

Terentyev D, Viatchenko-Karpinski S, Valdivia HH, Escobar AL & Györke S (2002). Luminal Ca^{2+} controls termination and refractory behavior of Ca^{2+}-induced Ca^{2+} release in cardiac myocytes. *Circ Res* **91**, 414–420.

Wang S, Liu Q, Zhu E, Porikli F & Yin J (2018). Hyper-parameter selection of one-class support vector machine by self-adaptive data shifting. *Pattern Recognit* **74**, 198–211.

Wang SQ, Song LS, Lakatta EG & Cheng H (2001). Ca^{2+} signalling between single L-type Ca^{2+} channels and ryanodine receptors in heart cells. *Nature* **410**, 592–596.

Wang YY, Mesirca P, Marqués-Sulé E, Zahradníková A, Villejoubert O, D'Ocon P, Ruiz C, Domingo D, Zorio E, Mangoni ME, Benitah J-P & Gómez AM (2017). RyR2^{R420Q} catecholaminergic polymorphic ventricular tachycardia mutation induces bradycardia by disturbing the coupled clock pacemaker mechanism. *JCI Insight* **2**, 1281.

Zahradnikova Jr A, Rizzetto R, Boncompagni S, Rabesahala de Meritens C, Zhang Y, Joanne P, Marques Sule E, Aguilar-Torres Y, Fernandez-Tenorio M, Villejoubert O, Li L, Wang YY, Mateo P, Nicolas V, Gerbaud P, Lai FA, Perrier R, Alvarez JL, Niggli E, Valdivia HH, Valdivia Carmen R, Ramos-Franco J, Zorio E, Zissimopoulos S, Protasi F, Benitah JP, Gomez AM (2021) Impaired Binding to Junctophilin2 and Nanostructural Alteration in CPVT Mutation. *Circulation Research*, **129**(3), e35–e52. http://doi.org/10.1161/circresaha.121.319094.

Zahradníková A Jr, Poláková E, Zahradník I & Zahradníková A (2007). Kinetics of calcium spikes in rat cardiac myocytes. *J Physiol* **578**, 677–691.

Zipfel WR, Williams RM & Webb WW (2003). Nonlinear magic: multiphoton microscopy in the biosciences. *Nat Biotechnol* **21**, 1369–1377.

Additional information

Data availability statement

Author's present address

H. Agarwal: Hitesh Agarwal, School of Pharmacy, South University, Savannah, GA, USA

Competing interests

The authors declare that they have no competing interests.

Author contributions

All of the experiments were performed at the Department of Physiology at the University of Bern. E.N., R.J., G.C.R.E.D., M.E. and A.M.G. conceived and designed the study. H.A. and G.C.R.E.D. developed the new caged compound. A.M.G. engineered the transgenic mouse model used for validation. R.J. acquired and analysed the data. R.J., E.N. and G.C.R.E.D. interpreted the data and drafted the manuscript. All authors revised the manuscript and provided intellectual feedback. All authors have read and approved the final version of this manuscript and agree to be accountable for all aspects of the work in ensuring that questions related to the accuracy or integrity of any part of the work are appropriately investigated and resolved. All persons designated as authors qualify for authorship, and all those who qualify for authorship are listed.

Funding statement

Acknowledgements

Keywords

Supporting information

Additional supporting information can be found online in the Supporting Information section at the end of the HTML view of the article. Supporting information files available:

Supplemental Table 1. Numbers of triggered second Ca^{2+} events in pairs in different experimental conditions.
Statistical Summary Document
Peer Review History